International Journal of Thermophysics, Vol. 16, No. 5, 1995

Measurements of the Isochoric Heat c_v at the Critical Point of SF_6 Under Microgravity: Results of the German Spacelab Mission D2[1]

J. Straub,[2,3] A. Haupt,[2] and L. Eicher[2]

During the Second German Spacelab Mission D2 (April 26 to May 6, 1993) the isochoric specific heat c_v of SF_6 was measured along the critical isochore under microgravity conditions with a newly developed scanning radiation calorimeter. This calorimeter provided the possibility to perform comparable heating and cooling runs with variable ramp rates since the spherical sample cell was heated and cooled only by radiation. During the experimental time of 220 h, 11 heating and cooling runs with different ramp rates were performed in a temperature range of $T - T_c = \pm 6$ K. Approaching T_c by cooling from the homogeneous one-phase region avoided significant temperature and density gradients in the fluid, which would have distorted the integral measurement of c_v. The inhomogenities introduced by a finite ramp rate were greatly reduced by the fast dynamic temperature propagation ("critical speeding up"). The c_v data achieved with slow cooling runs are in remarkably good agreement with the theoretical prediction more than one order of magnitude closer to the critical point than any c_v measurements done so far. The preliminary value for the critical exponent α is 0.107 ± 0.02, and for the amplitude ratio we obtained $A^-/A^+ = 1.94 \pm 0.07$. In contrast to the cooling runs, the heating runs showed a strong hysteresis of c_v. A comparison to $1g$ measurements is provided.

KEY WORDS: critical phenomena; isochoric heat capacity; microgravity; sulfur hexafluoride.

[1] Invited paper presented at the Twelfth Symposium on Thermophysical Properties, June 19–24, 1994, Boulder, Colorado, USA.

[2] Lehrstuhl A für Thermodynamik, Technische Universität München, Arcisstr. 21, 80333 München, Germany.

[3] To whom correspondence should be addressed.

0195-928X/95/0900-1033$07.50/0

1. INTRODUCTION

The isochoric heat capacity c_v of a fluid system is generally determined by the measurement of the total amount of heat input to the sample and the resulting temperature increase. Consequently the obtained value represents the integral value over all fluid states existing in the sample volume. Gradients in density and temperature in the fluid cause errors in the attempt to obtain true ("real") values of c_v. This is particularly relevant close to the critical point of a pure fluid. Performing very slow heating ramps indeed ensures the minimization of temperature gradients in the bulk fluid, but due to the high compressibility of the fluid, the hydrostatic pressure causes a strong density stratification which distorts the c_v measurement. To overcome this problem the first experiment under microgravity (μg) conditions was performed during the first German Spacelab Mission D1 in 1985. However, the measured c_v values were even more strongly distorted than those obtained with the same facility and the same ramp rates under $1g$ conditions. The interpretation of these results was found in a delayed density equilibration during heating up of the sample from the two-phase region through the critical temperature (T_c). We suspect that this was caused by the slow mass transport by a diffusion process from the liquid to the vapor phase near the critical point. This phenomenon became important under reduced gravity since there the wetting conditions caused a different phase distribution with longer diffusion lengths in the cell than on earth (for details see Refs. 1 and 2).

The understanding of this effect together with the observation of a fast temperature propagation even under μg conditions observed during a TEXUS rocket experiment [3] initiated the development of a new calorimeter method where c_v is determined in cooling runs. Doing this, the fast temperature propagation should have provided a nearly isothermal bulk fluid without gravity-driven density stratification near T_c. In this non-adiabatic scanning radiation calorimeter the sample cell was heated and cooled only by radiation heat exchange between the cell and the surrounding shell. The cell was equipped with four thermistors at different radial positions to measure the temperature distribution in the fluid during heating and cooling runs and to receive information about the heat transport in the fluid. After the successful tests of the new calorimeter on earth, the question arose whether this concept represented the right track to get closer to the critical point than was previously possible. We received the affirmative answer during the Second German Spacelab Mission D2, from April 26 to May 6, 1993.

2. SCIENTIFIC OBJECTIVES

The main objective of this investigation is to measure the "real" behavior of c_v at the critical density of a pure fluid (here SF_6) in the immediate vicinity of the critical point, where measurements done so far were distorted by an inhomogeneous density distribution. From the results the universal values for the critical exponent α and the amplitude ratio A^-/A^+ for a system of the 3,1-class are derived. Furthermore, the extension of the "asymptotic region" for pure SF_6 will be determined. The second motivation for this experiment is to explain the unexpected results obtained during the D1 mission by measuring c_v during both cooling and heating ramps. Additional experiments were performed in a pulse heating mode to investigate systematically fast dynamic temperature propagation, called "critical speeding up" [4] or "piston effect" [5]. These experiments are reported in detail in Refs. 6 and 7. Finally, our measurement, performed in the region of $-6 < T - T_c < +6$ K on the critical isochore of SF_6 may contribute to the improvement of the equation of state [8]. Due to its convenient critical parameters SF_6 has become well established as a model fluid for basic experiments at the critical point under both μg and $1g$ conditions.

3. MEASURING CONCEPT AND DATA EVALUATION

3.1. Construction of the Calorimeter

Due to the space limitations the description of the apparatus is rather short; for detailed information see Ref. 9. To realize the new measuring concept of heating and cooling the sample by radiation, the high-precision thermostat (HPT), already flown on the D1 mission, was used in a modified form. In particular, instead of the coin-shaped D1 cell, with a diameter of 30 mm and a height of 1 mm, a spherical cell of 20-mm diameter was used (Fig. 1). This geometry provided symmetrical boundary conditions for the mass and temperature distribution in the fluid. The sphere was obtained by electrolytical coating of an aluminium core with gold and copper and subsequent dissolving of the core with acid. A wall thickness of only $s = 0.4$ mm ensured a high rigidity of $(\Delta V/V)/dp = 0.005\ \text{bar}^{-1}$ and a small heat capacity C_c of the empty cell. This gave values for the ratio of the fluid capacity C_{fluid} and the total cell capacity C_{tot} of $(C_{\text{Fluid}}/C_{\text{Tot}}) \times 100 = 83\%$ at $T = T_c - 0.1$ K and of $(C_{\text{Fluid}}/C_{\text{Tot}}) \times 100 = 76\%$ for $T = T_c + 0.1$ K. The sample density was adjusted to $\rho = 737.2 \pm 2\ \text{kg} \cdot \text{m}^{-3}$ according to Ref. 10,

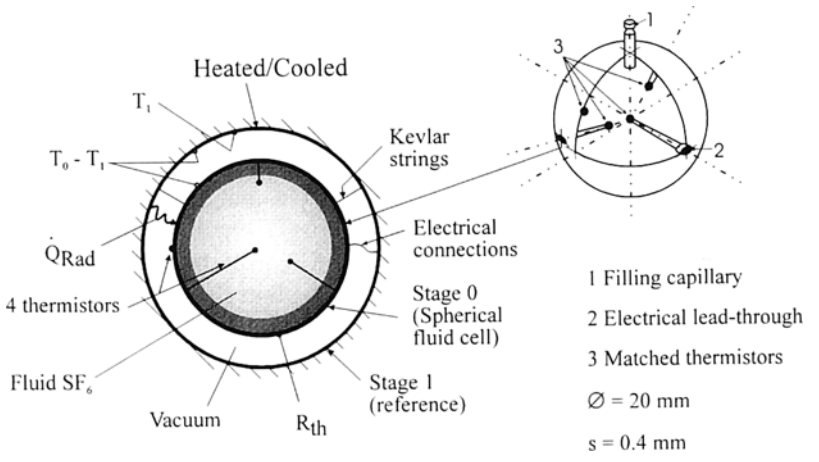

Fig. 1. Schematic setup of the new scanning radiation calorimeter. The spherical cell (stage 0) is heated/cooled by heat exchange with the surrounding shell (stage 1) by radiation ($\dot{Q}_{rad}$). To minimize heat transport by conduction, the thermostat is evacuated; the connections between the stages are done with Kevlar strings and special electrical connections. The specific heat is determined by measurement of $T_0 - T_1$ and T_1. The sample cell has a diameter of 20 mm and a wall thickness of 0.4 mm. Four thermistors are used to monitor the temperature distribution in the cell.

which determined the critical density of SF_6 to be $\rho_c = 737.0 \pm 7\ \mathrm{kg \cdot m^{-3}}$. The sample purity measured by the producer of the fluid used for this investigation was 99.998%.

3.2. Derivation of c_v from the Measurement

The heat capacity was obtained by determination of the amount of heat exchange between the cell (stage 0) and the surrounding shell (stage 1) and the resulting heating/cooling rate of the cell dT_0/dt. This was realized by measurement of the temperature difference $T_0 - T_1$ and determination of the temperature T_1. For the case of small temperature differences between T_0 and T_1, the Boltzmann equation of heat radiation can be linearized by introducing the thermal resistance R_{th}, which depends on the absolute value of T_0 and T_1. To minimize heat transport by conduction, the entire calorimeter was evacuated with an ion getter pump and the cell was fixed in stage 1 by Kevlar strings. The resistance R_{th} includes coefficients both for radiation and for the small amount of heat exchange by conduction through the mechanical and electrical connections. The value of R_{th} was experimentally determined. With that, c_v could be deduced:

$$c_v = \left(\frac{(1/R_{th})(T_0 - T_1) - P_{th}}{d[(T_0 - T_1) + T_1]/dt} - C_c \right) \left(\frac{1}{m_{sample}} \right) \tag{1}$$

where P_{th} is the heat input to the cell by the thermistor, C_c is the heat capacity of the empty cell, and m_{sample} is the mass of the sample fluid. For the results presented here we used an estimated value of C_c since the cell will be emptied only after finishing the reference tests in the lab.

3.3. Ramp Methods

Two types of cooling/heating ramps could be realized.

- Cooling/heating of stage 1 with a constant ramp rate was performed by controlling the temperature difference between stage 2 and stage 1 to be a constant value. During both cooling and heating runs the cell followed this ramp without controlling, only heated or cooled by radiation heat exchange.

- To save time during the mission, quasi-exponential cooling/heating modes with a decreasing ramp rate approaching the critical point were performed. This was done regarding the diverging time constant for reaching thermodynamic equilibrium and the fact of the increasing gradient of $(\delta c_v/\delta \rho)_p$ at the critical point. The outer stage 3 was used as a heat sink/source by controlling the temperature T_3 at a certain level below/above T_c. The inner stages 0, 1, and 2 were cooled down by radiation heat transfer without any controlling, which gave a quasi-exponential cooling ramp for these stages. The resulting ramp rate of the cell at T_c could be chosen by choosing the value of T_3. During the slowest cooling runs

Table I. Cooling and Heating Ramps Performed During the D2 Mission

Run No.	Ramp rate ($K \cdot h^{-1}$)	Temperature range (K)
1	Constant, −2.0	$+6 < T - T_c < -2$
2	Constant, −1.3	$+5 < T - T_c < -6$
3	Constant, −0.9	$+3 < T - T_c < -5$
4	Constant, −0.4	$+5 < T - T_c < -3$
5	Quasi-exponential, $-0.5 \cdots -0.06$	$+3 < T - T_c < -6$
6	Quasi-exponential, $-0.5 \cdots -0.06$	$+3 < T - T_c < -0.2$
7	Constant, +2.0	$-1.5 < T - T_c < +4.5$
8	Constant, +2.0	$-6 < T - T_c < +3$
9	Constant, +1.3	$-6 < T - T_c < +6$
10	Constant, +0.4	$-3 < T - T_c < +3$
11	Quasi-exponential, $+2.0 \cdots +0.04$	$-6 < T - T_c < +0.1$

(Nos. 5 and 6 in Table I) the cell was cooled with $dT_0/dt = -0.06\ \mathrm{K \cdot h^{-1}}$ through the critical point. During the slowest heating run (No. 11 in Table I) the cell was heated with $dT_0/dt = +0.04\ \mathrm{K \cdot h^{-1}}$ through the critical point.

3.4. Temperature Measurement

To observe the heat flow in the bulk fluid during the ramps one thermistor on the outer surface of the wall and three thermistors at different radii in the bulk were installed in the cell. Due to technical restrictions, and to minimize the dissipated heat input to the fluid, only one sensor was active at any time. After an active period of 2 min, made necessary by the 3.9-s time constant of the lock-in amplifier (LIA), the next sensor was activated. The resulting gaps in the temperature course of each sensor were filled by numerical interpolation. Due to the integration time of the LIA, small divergences between the resistance curves of the different sensors caused a transient deviation of the signal level after changing the sensor even when there was no temperature difference between the sensors. To avoid this problem during the crossing of T_c the sensor scanning was switched off when $|T - T_c| < 0.3$ K. To determine the sensor drift four calibration runs at different temperature levels were conducted during the mission. Artificial aging of the thermistors performed before their selection for the flight hardware reduced the drift rate to $\Delta T/t < 1\ \mathrm{mK \cdot year^{-1}}$. Two Pt25 sensors installed in stage 1 survived the vibrations of the shuttle liftoff and could be used as the temperature reference for the calibration.

4. THE D2 EXPERIMENT

The experiment HPT-HYDRA was flown on board the Space Shuttle Columbia STS 55 during the Second German Spacelab Mission D2. Since the HPT is a single-user facility with low energy consumption, we got nearly 9 days of experimental time. Seven days was used for heat capacity measurements, and during 2 days investigations of fast temperature propagation in near-critical fluids were conducted. Due to the configuration of the data interface between HPT and the Spacelab system, the data rate was fixed to 1.6 Hz, which was sufficient for the c_v measurements, although a higher rate would have reduced the uncertainty of the dynamic measurements. The large amount of data (about 500 Mbyte during 9 days) was evaluated online with our own hard- and software at the mission control center in Oberpfaffenhofen near Munich. This gave us the possibility to react directly to experimental results or problems by changing the original timeline. Additional inputs needed by the HPT, like the start of a new experiment run or the change of software parameters, were done manually by the astronaut team.

5. RESULTS AND DISCUSSION

During D2 we performed several heating and cooling runs (see Table I) to measure c_v around the critical point and to investigate the hysteresis between both modes. Due to space limitations we point out the results only from selected runs.

5.1. Cooling Ramps under μg

Figure 2 shows a log–log plot of the specific heat c_v of SF_6 versus the reduced temperature $\tau = (T - T_c)/T_c$ measured along the critical isochore under μg conditions during a cooling run with a constant ramp rate of $dT_0/dt = -0.4\ \mathrm{K} \cdot \mathrm{h}^{-1}$ (run 4). To investigate the influence of the ramp rate on the measurement of c_v, these data are compared to data computed for

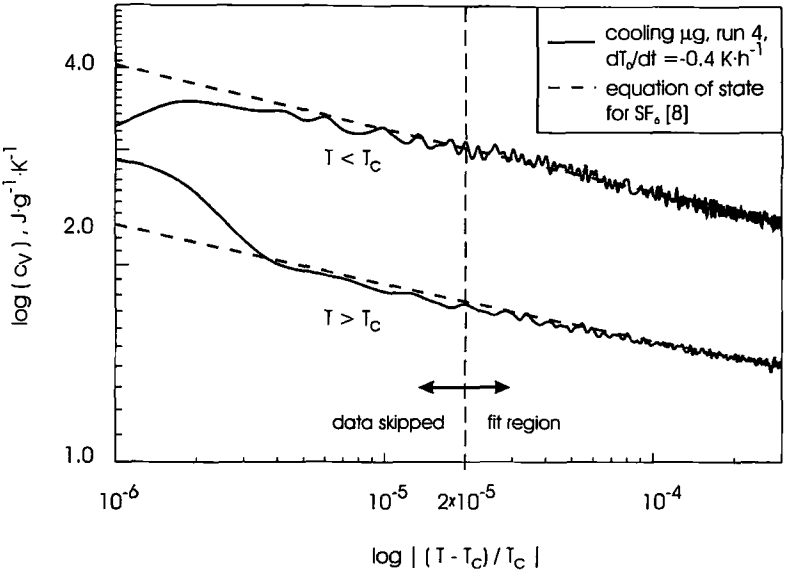

Fig. 2. Double-logarithmic plot of the isochoric specific heat c_v of SF_6 at critical density as a function of the reduced temperature difference $\tau = |(T - T_c)/T_c|$ measured under μg during a cooling run with $dT_0/dt = -0.4\ \mathrm{K} \cdot \mathrm{h}^{-1}$ (run 4 in Table I). Due to the large number of data ($\approx$2700 values in the temperature region shown), instead of data points a smoothed spline representation of the data is used here. The dashed line represents data computed for SF_6 at critical density with the linear model equation of state of Ref. 8. This comparison reveals the influence of the ramp rate on the c_v data due to existing gradients in the temperature and density. In spite of the relatively fast ramp rate, a significant deviation is obvious only for $\tau < 2 \times 10^{-5}$ in the two-phase region and for $\tau < 6 \times 10^{-6}$ in the one-phase region. This range was skipped in the regression analysis.

SF_6 at critical density with the linear model equation of state of Ref. 8 (dashed line). It is clearly shown that in spite of the relatively fast ramp rate, the experimenal data deviate significantly only for $|\tau| < 6 \times 10^{-6}$ for $T > T_c$ and for $|\tau| < 2 \times 10^{-5}$ for $T < T_c$.

5.1.1. Temperature and Density Distribution During Cooling Ramps

With the data of run 4 we want to examine the reasons for the high precision of the c_v measurements taken while cooling the sample. The run started at $T = T_c + 5$ K after homogenization of the fluid by thermostating the sample for 6 h. Figure 3 shows the development of the temperature field measured by the four sensors in the sample fluid during the cooling phase with the constant ramp rate of $dT_0/dt = -0.4\ \mathrm{K} \cdot \mathrm{h}^{-1}$ (run 4). The dotted lines represent the computed temperature differences based on the effect of "critical speeding up," which includes temperature equilibration both by conduction and by isentropic heating [4]. The final calibration of the cell

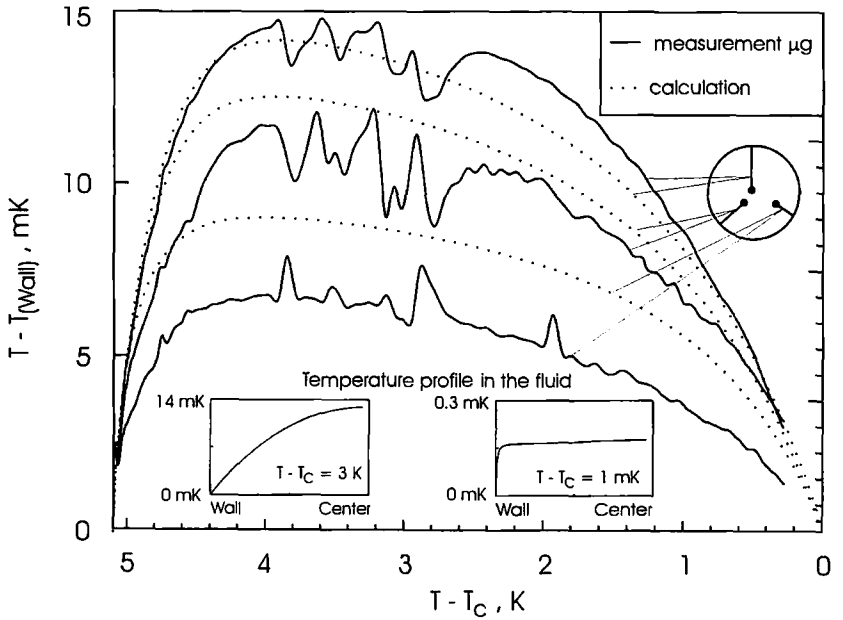

Fig. 3. Measured temperature differences in the sample fluid $T - T_{\mathrm{Wall}}$ (solid lines) during a cooling run of $dT_0/dt = -0.4\ \mathrm{K} \cdot \mathrm{h}^{-1}$ (run 4) from $T - T_c = +5$ K through the critical point in comparison to the computation including both heat conduction and the effect of isentropic heating (dotted lines). The calculated temperature profile in the sample between the wall and the center of the cell is given for $T - T_c = +3$ K and $T - T_c = +0.001$ K.

sensors has not been performed yet. The calculated and experimental values are clearly in qualitative agreement. The quantitative deviations may improve after the calibration. The maximum temperature difference between the wall and the center of the cell was about 14 mK at $T-T_c=+4$ K (obtained both by measurement and by calculation). Approaching the critical point the temperature difference clearly vanishes due to the increasing influence of isentropic heating. At $T-T_c=+0.25$ K the sensor scanning was deactivated, and therefore there are no experimental data in this region. The numerical calculation yields that the temperature difference between wall and center decreased to about 0.2 mK at $T-T_c=+0.001$ K.

In addition, the data are consistent with the calculation which shows (see insets in Fig. 3) that at $T-T_c=+3$ K, a fully developed temperature profile existed which is similar to a temperature profile caused only by heat conduction. Near T_c the calculation shows that the increasing influence of isentropic heating resulted in a very thin boundary layer with a temperature difference of 0.15 mK and a nearly isothermal bulk fluid.

The phase transition during cooling down in the 2-phase appears to have been carried out without the generation of significant inhomogenities in the density and temperature of both the vapor and the liquid phase, as explained in detail in Refs. 6 and 7. This indicates that the heat and mass transfer occurred undelayed due to the existence of a dispersion of small droplets and bubbles during cooling down in the two-phase region. This phenomenon has been observed in several experiments under μg conditions, i.e., in our TEXUS experiment [3], during the IML-1 Mission in the Critical Point Facility (CPF) by the group of Wilkinson and by the group of Beysens [12], and during the USMP-2 Mission in the experiment ZENO by the group of Gammon [13].

5.1.2. Influence of Inhomogenities on the Specific Heat

What is the influence of such temperature and density gradients on the integral measurement of c_v? We examine this for run 4 with a constant cooling rate of $-0.4\ \mathrm{K}\cdot\mathrm{h}^{-1}$. In the region of the largest temperature differences in the cell (between 4.5 and 1 K above T_c), the isobaric expansion coefficient $(\delta\rho/\delta T)_p$ is small, which gives a negligible difference between the density at the wall and that at the center of the cell. Integrating over all fluid states for a temperature difference of 10 mK and the corresponding density gradient by using the equation of state of Ref. 8 gives a difference between the c_v data of the inhomogeneous fluid and the value of the homogeneous fluid of $(c_{v,\,\mathrm{inhom}}-c_{v,\,\mathrm{hom}})/c_{v,\,\mathrm{hom}}\times 100=0.1\%$ at $T-T_c=+1$ K. The deviation at $T-T_c=+0.001$ K and a temperature difference between the wall and the center of 0.2 mK is about $(c_{v,\,\mathrm{inhom}}-c_{v,\,\mathrm{hom}})/c_{v,\,\mathrm{hom}}\times 100=0.65\%$. All cooling runs showed similar behavior of decreasing

temperature gradients and significant change of the form of the temperature profile. The comparison between the simulation of runs with different ramp rates showed that the resulting deviation of c_v is nearly proportional to the ramp rate. This means that the deviation for the slowest runs (runs 5 and 6) is $(c_{v,\,\mathrm{inhom}} - c_{v,\,\mathrm{hom}})/c_{v,\,\mathrm{hom}} \times 100 \approx 0.1\,\%$ at $T - T_c = +0.001$ K. The observed deviation of the c_v data is consistent with the calculated values based on the measured and calculated temperature profiles in the fluid above T_c.

5.1.3. Regression Analysis

It must be mentioned that the final calibration of the flight hardware, including the calibration of the temperature sensors and the precise determination of the capacity of the emptied test cell, has not yet been performed due to the late return of the flight hardware to our lab and the necessity of additional reference tests on earth. Therefore the following results should be regarded as preliminary.

Figure 4 shows the c_v data of the quasi-exponential cooling run of $dT_0/dt = -0.006\ \mathrm{K \cdot h^{-1}}$ in a log–log plot versus the reduced temperature τ. To find the influence of the ramp rate for this run the data were compared to the same data used for the comparison of run 4 (see Section 5.1). The departure of c_v from this curve due to remaining gradients in the fluid increases only in a region of $|\tau| < 3 \times 10^{-6}$, which was skipped for the regression analysis. To exclude any biasing no averaging of the data was used except for spline smoothing of the temperature T_1. Fitting the entire data set in a region of $3 \times 10^{-6} < |\tau| < 4 \times 10^{-4}$ (about 18000 data points!) by the simple power law

$$c_v = A^{-/+} |\tau|^{-\alpha} + B \tag{2}$$

gives values for the universal exponent $\alpha = 0.107 \pm 0.02$ and the amplitude ratio $A^-/A^+ = 1.94 \pm 0.07$. These are in very good agreement with values of high-precision experiments in $1g$ and theoretical values obtained from numerical calculations of the renormalization group theory (see Table II). Since the final calibration has not been performed, no absolute value for the critical temperature of the D2 sample can be given yet, but the well-defined peak of the c_v data at the critical point yields an uncertainty of the relative temperature difference $T - T_c$ of only ± 0.4 mK for both run 5 and run 6. In the analysis T_c was varied in this range, resulting in the given uncertainties of the values of α and A^-/A^+.

The data of run 4 ($dT_0/dt = -0.4$ K/h) was fitted in a broader region around T_c. As mentioned before, the data of this run show a deviation between $-6\ \mathrm{mK} < T - T_c < +2\ \mathrm{mK}$, which was excluded in the regression

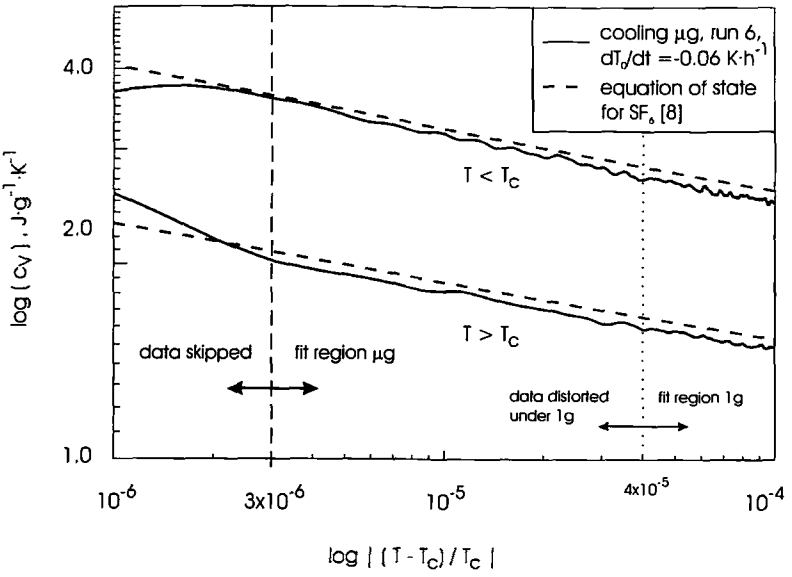

Fig. 4. Double-logarithmic plot of the isochoric specific heat c_v of SF_6 at critical density as a function of the reduced temperature difference $\tau = |(T - T_c)/T_c|$ measured under μg during a cooling run with a quasi-exponential ramp rate (run 6 in Table I). The sample was cooled with $dT_0/dt = -0.06\ \mathrm{K \cdot h^{-1}}$ through the critical point. Due to the large number of data (≈ 6000 values in the shown temperature region), instead of data points a smoothed spline representation of the data is used here. The comparison with data of the equation of state as used in Fig. 2 (dashed line) reveals the influence of the ramp rate on the c_v data due to gradients in the temperature and density in the fluid. A significant deviation is obvious only for $\tau < 3 \times 10^{-6}$ both in the two-phase region and in the one-phase region. This range was skipped in the regression analysis. The values obtained by the regression analysis were $\alpha = 1.07 \pm 0.02$ for the critical exponent and $A^-/A^+ = 1.94 \pm 0.07$ for the amplitude ratio. Specific heat data of pure fluids measured on earth, i.e., by investigators in Refs. 2 and 18, showed a significant distortion in the region of $|\tau| < 4 \times 10^{-5}$ due to strong density stratifications caused by the diverging compressibility.

analysis. Fitting these data to the extended power law suggested by renormalization group predictions,

$$c_v = A^{-/+} |\tau|^{-\alpha} (1 + D^{-/+} |\tau|^{\Delta}) + B + E \cdot |\tau| \tag{3}$$

in the region of $2 \times 10^{-5} < |\tau| < 2 \times 10^{-3}$ yields the critical exponent $\alpha = 0.107 \pm 0.025$ and the amplitude ratio $A^-/A^+ = 1.90 \pm 0.08$. For this analysis the universal exponent Δ was fixed to the theoretical value 0.5. The uncertainty (about ± 0.6 mK) of the relative temperature $T - T_c$ for this run was taken from the c_v data.

Table II. Comparison of Curve Fitting in this Work and Previous Experimental and Theoretical Results

System	Approximation equation	Interval of fit $\tau=(T-T_c)/T_c$	α	A^-/A^+	Reference(s)
SF_6	$c_v = A^{-/+}\lvert\tau\rvert^{-\alpha} + B$	$3.0\times10^{-6} < \lvert\tau\rvert < 5.0\times10^{-4}$	0.107 ± 0.02	1.94 ± 0.07	this work
SF_6	$c_v = A^{-/+}\lvert\tau\rvert^{-\alpha} + B$	$5.0\times10^{-5} < \lvert\tau\rvert < 1.6\times10^{-3}$	0.1075 ± 0.005	1.86 ± 0.06	[1, 2]
CO_2	$c_v = A^{-/+}\lvert\tau\rvert^{-\alpha} + B$	$4.0\times10^{-5} < \lvert\tau\rvert < 4.5\times10^{-4}$	0.1084 ± 0.0023	1.965 ± 0.03	[17]
3EA–D_2O	$c_v = A^{-/+}\lvert\tau\rvert^{-\alpha}(1 + D^{-/+}\lvert\tau\rvert^{d}) + B + E\lvert\tau\rvert$	$7.0\times10^{-6} < \lvert\tau\rvert < 6.0\times10^{-4}$	0.107 ± 0.002	1.75 ± 0.03	[18]
Renormalization group theory			0.110 ± 0.005	$1.82 - 2.08$	[11, 19–21]

5.2. Heating Ramps Under μg

The measurements of c_v during the heating runs under μg conditions yielded a totally different behavior, which is examined with the results of runs 10 and 11. Figure 5 shows the hysteresis of c_v between a cooling run with a ramp rate of $dT_0/dt = -0.4\ \mathrm{K \cdot h^{-1}}$ (run 4) and a heating run of $dT_0/dt = +0.4\ \mathrm{K \cdot h^{-1}}$ at T_c (run 10). The c_v data in the two-phase region were significantly lower than those from the cooling run, there was no singularity of c_v at T_c, and the c_v course was very irregular in the two-phase region.

The hysteresis of c_v became obvious at about $T - T_c = -0.4$ K and increased with decreasing distance of T_c. This observation of a significant lower c_v course while heating the sample is similar to that of the D1 Mission reported in Ref. 1. There the interpretation is based on a fast temperature relaxation caused by the effect of isentropic heating and a delayed density equilibration by diffusion with an vanishing diffusion coefficient at the critical point. As predicted by Onuki and Ferell [14] and measured by Straub et al. [6, 7], the effect of isentropic heating causes a significant temperature difference between liquid and vapor in a near-critical two-phase system. Current calculations [15] show that the equilibration of this temperature difference is extremely slowed down by the delayed mass transport

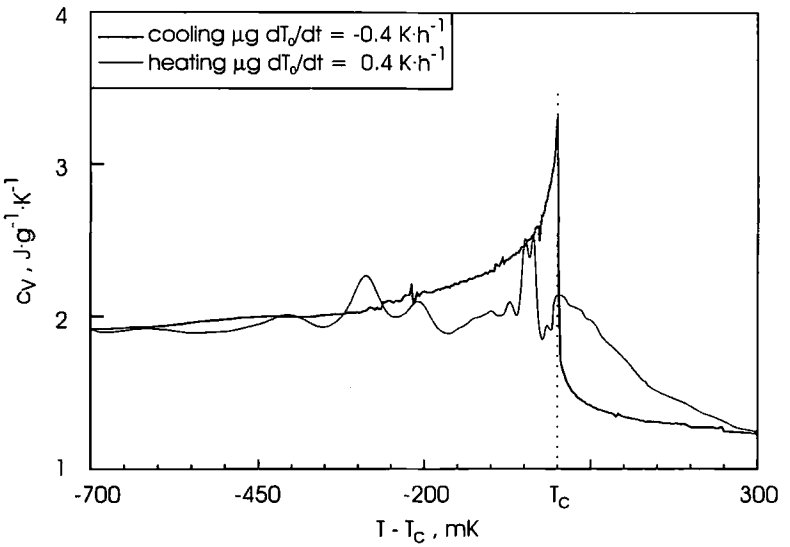

Fig. 5. Hysteresis between the c_v course obtained by a cooling run with $dT_0/dt = -0.4\ \mathrm{K \cdot h^{-1}}$ (thick line) and that by a heating run with $dT_0/dt = +0.4\ \mathrm{K \cdot h^{-1}}$ (thin line) measured under μg (for details see text).

across the interface. Since the interface in the flat D1 cell was much smaller for the μg measurements than for the $1g$ measurements due to the wetting conditions, it might be possible to explain the D1 results with this model. In contradiction to the prediction, no significant temperature differences were measured in the D2 cell while heating in the two-phase region. This could happen if the three thermistors in the cell were totally covered by the liquid phase caused by the effect of critical wetting investigated in [16]. To give quantitative statements with the D2 data further evaluation is necessary.

Considering the inhomogenities in the fluid caused by the effect of isentropic heating, it is clear that the heating runs could not show any peak of c_v crossing the critical temperature. Instead of the singularity the c_v course was flattened out around T_c. In the one-phase region the temperature equilibration became faster due to the missing interface. At $T - T_c = +0.3$ K the fluid was equilibrated again and the c_v data corresponded to those of the nearly homogeneous fluid of the cooling run again.

Second, the course of the wall temperature indicated small jumps of some millikelvins around the average ramp rate. Differentiating this irregular course of the cell temperature T_0 to obtain c_v [see Eq. (1)] resulted in the observed scatter in Fig. 5. Our tentative explanation for these jumps is that the boundary layer at the cell wall was temporarily superheated and nucleation pool boiling occurred. The energy necessary for the evaporation was taken from the cell wall, resulting in the sudden decrease in the ramp rate of the wall temperature.

5.3. Experiments Under $1g$

The results of c_v measurements performed with the new calorimeter under earth gravity conditions should be mentioned here. The c_v data obtained during heating also showed a significant hysteresis compared to the cooling runs (Fig. 6), and this hysteresis was proportional to the ramp rate. Increasing the heating ramp rate caused a stronger deviation of c_v in the two-phase region and the course was more flattened out around the critical point. In contrast to the μg data, the $1g$ data were much more regular since any superheating of the boundary layer might have been suppressed by the mixing effect of buoyancy convection.

However, cooling runs with different ramp rates revealed nearly the same c_v course in the one-phase region above T_c. The inset in Fig. 6 shows that c_v obtained by cooling ($dT_0/dt = -0.4\ \mathrm{K \cdot h^{-1}}$) under $1g$ had nearly the same behavior as the cooling runs performed under μg (represented by the fit curve of cooling run 6 with $dT_0/dt = -0.06\ \mathrm{K \cdot h^{-1}}$). Obviously no significant temperature and density gradients were created above T_c in

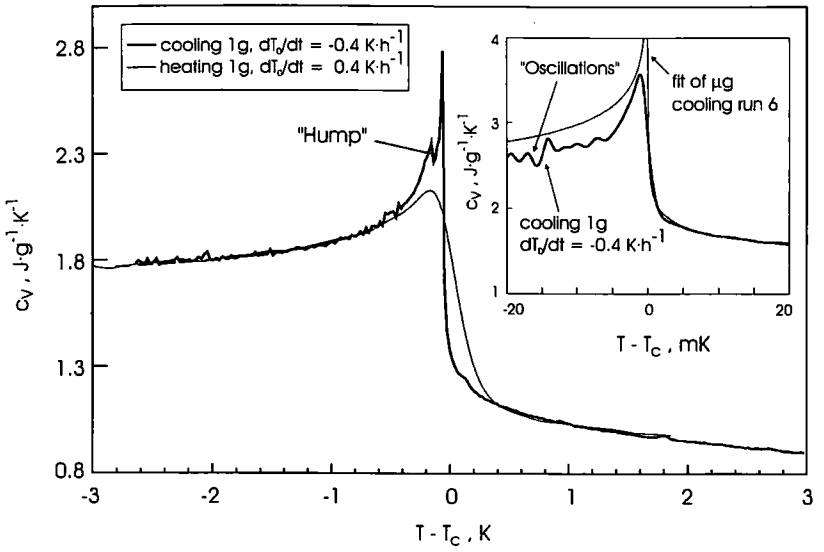

Fig. 6. Hysteresis between the c_v course obtained by a cooling run with $dT_0/dt = -0.4\ \mathrm{K} \cdot \mathrm{h}^{-1}$ (thick line) and that by a heating run with $dT_0/dt = +0.4\ \mathrm{K} \cdot \mathrm{h}^{-1}$ (thin line) measured under 1 g. The inset shows a comparison between c_v data obtained with this cooling run and the fit representation of the μg data obtained with the quasi-exponential cooling run with $dT_0/dt = -0.06\ \mathrm{K} \cdot \mathrm{h}^{-1}$ (for details see text).

spite of the comparable fast ramp rate and the large hydrostatic height of our cell (20 mm).

The behavior of c_v during cooling into the two-phase region revealed the effect of an oscillation of the cell temperature for some minutes just below T_c. This oscillation may have been a result of periodic subcooling and subsequent condensation of a part of the vapor, with an abrupt release of latent heat. In general, c_v remained lower in the two-phase region than calculated for the equilibrated fluid until a significant "hump" occurred, whereupon c_v returned to the equilibrium course. Since one part of c_v represents the latent heat for the density change, a delayed density equilibration during phase separation may be the reason for this irregularity of the c_v course.

6. CONCLUSION

Using the new scanning radiation calorimeter under μg conditions, the specific heat c_v of pure SF_6 was measured in the region of $T - T_c = \pm 6$ K. Approaching T_c from the one-phase region avoided strong initial gradients

in the fluid, and the temperature and density gradients introduced by a finite ramp rate were greatly reduced by the effect of isentropic heating. The phase separation below T_c occurred undelayed due to the existence of a dispersion of small droplets and bubbles. The data set obtained by a quasi-exponential cooling ramp with $dT_0/dt = -0.06\ \mathrm{K} \cdot \mathrm{h}^{-1}$ at the critical point agreed with the theoretical model after the data of $|\tau| < 3 \times 10^{-6}$ was excluded from the regression analysis. The obtained values for the universal critical exponent and amplitude ratio are $\alpha = 0.107 \pm 0.02$ and $A^-/A^+ = 1.94 \pm 0.07$, respectively, which are in very good agreement with other investigations of 3,1-systems.

The c_v courses obtained by heating runs showed a strong hysteresis in comparison to the cooling runs. There was no critical singularity, but a significantly lower course in the two-phase region, which indicated a delayed equilibration of the fluid upon approaching T_c. Cooling runs performed under $1g$ conditions yielded good results for c_v in the one-phase region, but in the two-phase region the data deviated significantly from the equilibrium course. Heating runs under $1g$ also showed a hysteresis of c_v compared to the cooling runs.

Final results of this investigation as well as a complete data set of c_v on the critical isochore of SF_6 will be published soon.

ACKNOWLEDGMENTS

This research is supported by Deutsche Agentur für Raumfahrtangelegenheiten (DARA), Project Number 50 QV 8948. The authors are very grateful to all persons who contributed with their work to the success of the D2 experiment HPT-HYDRA. In particular, we want to thank the crew of the Space Shuttle Columbia STS 55, the responsible persons at the company Kayser-Threde, Munich, the operations control team of DLR and NASA, and all colleagues and students for their outstanding engagement.

REFERENCES

1. J. Straub and K. Nitsche, *Fluid Phase Equil.* **88**:183 (1993).
2. K. Nitsche, *Die isochore Wärmekapazität im kritischen Gebiet von SF_6 unter Erdschwere und reduzierter Schwere*, Thesis (Technical University Munich, Munich, 1990).
3. K. Nitsche, J. Straub, and R. Lange, *Scientific Report Aeronautics and Astronautics* (BMFT, 1984).
4. H. Boukari, J. N. Shaumeyer, M. E. Briggs, and R. W. Gammon, *Phys. Rev. A* **41**:2260 (1990).
5. B. Zappoli, D. Bailly, Y. Garrabos, B. LeNeindre, P. Guenon, and D. Beysens, *Phys. Rev. A* **41**:2264 (1990).
6. J. Straub, L. Eicher, and A. Haupt, *Int. J. Thermophys.* **16**:1051 (1995).

7. J. Straub, L. Eicher, and A. Haupt, *Phys. Rev. E* **51** (6) (1995).
8. A. Abbaci and J. V. Sengers, Technical Report No. BN 1111 (University of Maryland, College Park, 1990).
9. J. Straub, A. Haupt, and K. Nitsche, *Fluid Phase Equil.* **88**:123 (1993).
10. T. Michels, personal communication (1981).
11. J. C. Le Guillou and J. Zinn-Justin, *Phys. Rev. B* **21**:3976 (1980).
12. D. Beysens, personal communications (1992).
13. R. Gammon, personal communications (1994).
14. A. Onuki, A. Ferell, *Physica A* **164**:245 (1990).
15. J. Straub and L. Eicher, accepted for publication in *Phys. Rev. Lett.* (1995).
16. M. Moldover and R. Gammon, *J. Chem. Phys.* **80**:528 (1984).
17. T. J. Edwards, *Specific Heat Measurements Near the Critical Point of* CO_2 Thesis (University of Western Australia, 1984).
18. E. Bloemen, J. Thoen, and W. Van Dael, *J. Chem. Phys.* **73**:4628 (1980).
19. A. Aharony and P. C. Hohenberg, *Phys. Rev. B* **13**:3081 (1976).
20. M. Barmatz, P. C. Hohenberg, and A. Kornblit, *Phys. Rev. B* **12**:1947 (1975).
21. C. Bervillier, *Phys. Rev. B* **14**:4964 (1976).